Self-Healing of Selectively Reflected Airy Beam from Resonant Atoms

Li Li[1] Zhao Xiaoxia[1] Zhu Junfan[1] Li Yuanyuan[1] Zhang Yiqi[3]
Zhang Yanpeng[3] Xu Kewei[1,2]

[1] *Institute of Applied Physics, Xi'an University of Arts and Science, Xi'an, Shaanxi* 710065, *China*
[2] *Nano-Film and Biological Materials Research Center, Xi'an Jiaotong University, Xi'an, Shaanxi* 710049, *China*
[3] *Key Laboratory for Physical Electronics and Devices of the Ministry of Education, Xi'an Jiaotong University, Xi'an, Shaanxi* 710049, *China*

Abstract Self-healing of selectively reflected (SR) Airy beam from cascade three-level atoms sandwiched between two dielectric walls is investigated. A theoretical model is developed to calculate SR Airy beam at an interface between dielectric and resonant atoms. Numerical simulation is also implemented, and the result shows that self-healed SR beams can be found both at normal and oblique incidence of the probe field, although there is a severe breakdown in the former case. We also show that the spectrum of the SR beams can be dramatically modified by the probe detuning and the coupling strength from the anisotropic behavior, enhancement and suppression of atomic radiation. The enhancement and the suppression are mainly from the interference and the alternating current (AC)-Stark splitting between dressed states created by the coupling field. These types of SR beams can have potential applications in the spatial detection and manipulation of resonant particles, as well as the optical storage and communication of information.

Key words laser optics; selective reflection spectroscopy; Airy beam; self-healing
OCIS codes 140.3295, 140.3300, 020.1670

共振原子选择反射艾里光束的自愈

李 莉[1] 赵小侠[1] 朱君凡[1] 李院院[1]* 张贻齐[3] 张彦鹏[3] 徐可为[1,2]

[1]西安文理学院 应用物理研究所，陕西 西安 710065
[2]西安交通大学 纳米薄膜与生物材料研究中心，陕西 西安 710049
[3]西安交通大学 电子物理与器件教育部重点实验室，陕西 西安 710049

摘要 研究了囚禁于两电介质面间级联三能级原子的选择反射(SR)艾里光束的自愈现象。建立了计算电介质与共振原子界面处艾里光束 SR 光谱的理论模型并进行了数值模拟。研究结果表明探测艾里光束在法向及斜入射的情形下其选择反射光束均表现出自愈行为，法向入射情形下出现了很大的间断。研究还发现，探测光的失谐量及耦合光的强度均可调制 SR 艾里光束的光谱，其调制来自于原子辐射的各向异性、增强或减弱。强耦合光产生的原子缀饰态相干效应及交流斯塔克效应是原子辐射增强或减弱的主要原因。这种 SR 艾里光束在共振粒子特性的空间探测、共振粒子的操控及光信息存储与通信等方面具有潜在的应用价值。

关键词 激光光学；选择反射光谱；艾里光束；自愈
中图分类号 O433 **文献标识码** A **doi**：10.3788/LOP50.121404

1 Introduction

An Airy beam can maintain resistance to diffraction and accelerating dynamics over several diffraction lengths before it is significantly distorted during the propagation[1-2]. Another feature of the Airy beam is its self-healing when perturbations are imposed on them[3-4]. These dynamic properties of Airy beams have

收稿日期：2013-06-28；**收到修改稿日期**：2013-08-18；**网络出版日期**：2013-11-12
基金项目：西安市科技计划(CXY1134WL02，CX12189WL02)
作者简介：李莉(1972—)，女，实验师，主要从事高分辨率光谱方面的的研究。E-mail：lilinxcn@aliyun.com
* **通信联系人**。E-mail：liyynxcn@aliyun.com

been shown in free space[5], electromagnetic induced transparency (EIT) atomic vapor[6], self-defocusing nonlinear medium[7], handed material[8] and an interface between two dielectric media[9]. A virtual source for generating an Airy wave has been identified to describe Airy beams[10]. It is also shown that the Airy beams can be used in the applications of beam trajectory controlling[11], particle manipulation[12], and plasma channel generation[13].

In this report, we examine the SR Airy beams radiated from cascade three-level cold atoms sandwiched between two dielectric walls. SR spectroscopy with its property of high resolution has been extensively used to study the resonant properties of a medium and atom-surface interaction at an interface[14-19]. The accelerating dynamics of the SR Airy beams can be modified by several factors, such as the incident angle, the detuning and the strength of the probe and the coupling beams. In our discussion, the coupling field under normal incidence is assumed. We show that the larger the incident angle of the probe field, the greater the accelerating rate of the SR beam. Self-healed SR beams can be found at both normal and oblique probe incidence, although there is a severe breakdown of that in the former case. We also show that the probe detuning and the coupling strength can dramatically modify the spectrum of the SR beams. This type of Airy beam can probably be used in the spatial detection and the manipulation of resonant particles.

2 Theoretical model

We consider a sample of atomic medium 2 sandwiched between two transparent dielectric windows 1 and 1′ (i.e., no absorptive or scattering losses) [Fig. 1(a)], situated respectively in the regions of $z<0$ and $z>L$. In such a confined atomic system, the spectrum of the electromagnetic field modes is strongly modified for wavelengths that are comparable with or larger than the physical dimensions. Due to the enhanced contribution of slow atoms, high resolution spectroscopy related to these confined atoms can be achieved, and used as a convenient tool in the study of atom-surface interaction[14-19]. A cascade three-level system in medium 2 is presented in Fig. 1(b), where the transition frequency of $|1\rangle-|2\rangle$ is ω_{21}, and that for $|2\rangle-|3\rangle$ is ω_{32}. The probe field $\boldsymbol{E}_p$ and the coupling field $\boldsymbol{E}_c$ applied to the system correspond to the transitions $|1\rangle-|2\rangle$ and $|2\rangle-|3\rangle$, respectively. $\omega_p(\omega_c)$, $\Delta_p=\omega_p-\omega_{21}(\Delta_c=\omega_c-\omega_{32})$ and $\boldsymbol{k}_p(\boldsymbol{k}_c)$ are the probe (the coupling) frequency, the detuning and the wave vector, respectively.

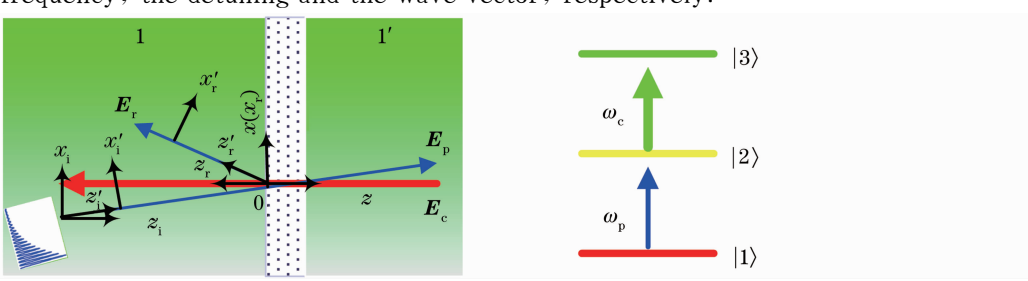

Fig. 1 (a) A sample of atoms confined between two transparent dielectric windows; (b) cascade three-level system of atoms

We restrict our discussion to the case that the probe field and the coupling field impinge at an incident angle θ_1 of the interface 1-2 and along the normal direction of the interface 1′-2, respectively. The amplitude of a paraxial probe beam can be written as

$$E_p(x_i,z_i=0)=u_0(x_i)\exp(ik_1\sin\theta_1 x_i) \tag{1}$$

where $u_0(x_i)=Ai(\pm x_i\cos\theta_1/x_0)\exp(\pm ax_i\cos\theta_1/x_0)$ is the transverse input field amplitude for a finite-power Airy beam, with a being the truncation and x_0 an arbitrary transverse scale. $k_1=n_1k_p$ is the probe wavenumber in medium 1 with dielectric constant ε_1 and refractive index $n_1=\sqrt{\varepsilon_1}$. The coordinate system $(x_i,z_i)=(x+s,z+h)$, with $s=h\tan\theta_1$ and $z=-h$ being the depth inside window 1.

When a Fourier transformation in coordinates (x, z) is applied to the probe field, $\boldsymbol{E}_p$ can be decomposed into many plane wave components $E_p^{(k)}$. Each Fourier component through the medium 2 yields the wave equation

$$\partial^2E_p^{(k)}(z)/\partial z^2+2iq_2\partial E_p^{(k)}(z)/\partial z=-4\pi q_2^2P^{(k)}(z), \tag{2}$$

where $q_2=\sqrt{k_p^2-k^2}$ is the z wavenumber of the Fourier component in the medium 2.

For simplicity, we assume that the second interface 2-1′ is antireflection coated; hence it is justified to assume that $[\partial E_p^{(k)}(z)/\partial z]_{z=L}\approx0$, and we obtain

$$[\partial E_p^{(k)}(z)/\partial z]_{z=0}=4\pi q_2^2\int_0^L P^{(k)}(z')\exp(2iq_2z')\mathrm{d}z'. \tag{3}$$

In Eqs. (2) and (3), the polarization $P^{(k)}(z) = N\mu_{21}\sigma_{21}^{(k)}(z)$, with N being the number density of atoms in the medium 2, and μ_{21} the transition dipole moment corresponding to $|1\rangle - |2\rangle$. The density matrix element σ_{21} can be obtained by solving the following coupled equations:

$$\partial\sigma_{32}/\partial t = \mathrm{i}G_{\mathrm{c}}(\sigma_{22}-\sigma_{33}) - \mathrm{i}G_{\mathrm{p}}^{(k)}\sigma_{31} - \Lambda_{32}\sigma_{32}, \tag{4a}$$

$$\partial\sigma_{21}/\partial t = \mathrm{i}G_{\mathrm{p}}^{(k)}(\sigma_{11}-\sigma_{22}) + \mathrm{i}G_{\mathrm{c}}\sigma_{31} - \Lambda_{21}\sigma_{21}, \tag{4b}$$

$$\partial\sigma_{31}/\partial t = \mathrm{i}G_{\mathrm{c}}\sigma_{21} - \mathrm{i}G_{\mathrm{p}}^{(k)}\sigma_{32} - \Lambda_{31}\sigma_{31}, \tag{4c}$$

where $\Lambda_{32} = \gamma_{32} - \mathrm{i}\Delta_{\mathrm{c}}$, $\Lambda_{21} = \gamma_{21} - \mathrm{i}\Delta_{\mathrm{p}}$, $\Lambda_{31} = \gamma_{31} - \mathrm{i}(\Delta_{\mathrm{c}} + \Delta_{\mathrm{p}})$; $G_{\mathrm{p}}^{(k)}$ and G_{c} are Rabi frequencies defined by $G_{\mathrm{p}}^{(k)} = \mu_{21}E_{\mathrm{p}}^{(k)}/\hbar$ and $G_{\mathrm{c}} = \mu_{32}E_{\mathrm{c}}/\hbar$, respectively, with μ_{32} being the transition dipole moment corresponding to $|2\rangle - |3\rangle$; γ_{ij} denotes the decay rate from level $|i\rangle$ to $|j\rangle$. For convenience, the superscript (k) in each density matrix element is omitted in Eqs. (4a)~(4c).

For a weak probe beam, we assume that the initial conditions are $\sigma_{11} \approx 1$, $\sigma_{22} \approx \sigma_{33} \approx 0$. Solving Eqs. (4a)~(4c), we obtain $\sigma_{21} = \mathrm{i}G_{\mathrm{p}}^{(k)}/\Lambda_{21} - \mathrm{i}G_{\mathrm{c}}^2G_{\mathrm{p}}^{(k)}/[\Lambda_{21}(\Lambda_{21}\Lambda_{31} + G_{\mathrm{c}}^2)]$, and the polarization can be written as

$$P^{(k)}(x,z) = \mathrm{i}N\mu_{21}G_{\mathrm{p}}^{(k)}(x,z)/\Lambda_{21} - \mathrm{i}N\mu_{21}G_{\mathrm{c}}^2G_{\mathrm{p}}^{(k)}(x,z)/[\Lambda_{21}(\Lambda_{21}\Lambda_{31} + G_{\mathrm{c}}^2)]. \tag{5}$$

The envelope function for the SR beam is given by the Fourier integral[8]

$$u(\chi_{\mathrm{r}}, z_{\mathrm{r}}) = \frac{1}{2\pi\cos\theta_1}\int_{-\infty}^{\infty}\mathrm{d}\kappa F_0\left(\frac{\kappa}{\cos\theta_1}\right)R_{\mathrm{sr}}(k_1\sin\theta_1+\kappa)\exp\left[\mathrm{i}\kappa\chi_{\mathrm{r}} - \mathrm{i}\frac{\kappa^2(z_{\mathrm{r}}+h)}{2k_1\cos^3\theta_1}\right], \tag{6}$$

where $\chi_{\mathrm{r}} = x_{\mathrm{r}} - z_{\mathrm{r}}\tan\theta_1$ is the reduced x coordinate at the propagation direction of the reflected beam along $x_{\mathrm{r}} = z_{\mathrm{r}}\tan\theta_1$ predicted by Snell's law; z_{r} is the distance of the SR beam from the interface 1-2 in medium 1. The Fourier transformation $F_0(k') = x_0\exp[\mathrm{i}(\pm k'x_0 + \mathrm{i}a)^3/3]$.

By applying boundary conditions at the interface, the SR coefficient of each component reads

$$R_{\mathrm{sr}}(k) = \mathrm{i}/[E_{\mathrm{pin}}^{(k)}(q_1+q_2)][\partial E_{\mathrm{p}}^{(k)}(z)/\partial z]_{z=0}, \tag{7}$$

where we assume that the probe field is s-polarized, $q_1 = \sqrt{k_1^2 - k^2}$ is the z wavenumber of the Fourier component in the medium 1. $E_{\mathrm{pin}}^{(k)}$ at the interface in the medium 1 can be defined by

$$E_{\mathrm{pin}}^{(k)} = \left[\int_{-\infty}^{\infty}E_{\mathrm{p}}(x,z)\exp(-\mathrm{i}kx)\mathrm{d}x\right]_{z=0}, \tag{8}$$

where

$$E_{\mathrm{p}}(x,z) = \frac{1}{2\pi}\int_{-\infty}^{+\infty}\left[\int_{-\infty}^{+\infty}E_{\mathrm{p}}(x,z=-h)\exp(-\mathrm{i}kx)\mathrm{d}x\right]\exp(\mathrm{i}kx)\exp[\mathrm{i}q_1(z+h)]\mathrm{d}k.$$

Substituting Eq. (5) into Eq. (3) and then into Eq. (7), one can obtain

$$R_{\mathrm{sr}}(k) = -\frac{4\pi q_2^2}{E_{\mathrm{pin}}^{(k)}(q_1+q_2)}\int_0^L\{N\mu_{21}G_{\mathrm{p}}^{(k)}(x,z')/\Lambda_{21} - N\mu_{21}G_{\mathrm{c}}^2G_{\mathrm{p}}^{(k)}(x,z')/[\Lambda_{21}(\Lambda_{21}\Lambda_{31}+G_{\mathrm{c}}^2)]\}\exp(2\mathrm{i}q_2z')\mathrm{d}z'. \tag{9}$$

The SR field represents the radiated waves propagating along the reflective direction from the macroscopic polarization of sandwiched atoms. Eqs. (6) and (9) evidently show that the spatial profile of the SR beam can be modulated by the SR coefficient R_{sr}, i.e., the atomic level structure, the thickness of atomic sample, as well as the incident angles, the detuning and the strengths of the probe and the coupling fields.

3 Results and discussion

Atomic parameters are chosen corresponding to a typical cascade three-level system in D_2 line of ^{87}Rb. The probe beam with a wavelength of 780 nm couples level $|1\rangle$ ($F = 2$, $5S_{1/2}$) to level $|2\rangle$ ($5P_{3/2}$), and level $|2\rangle$ to level $|3\rangle$ ($5D_{3/2}$) for the coupling beam with a wavelength of 776.16 nm. The decay rates are $\gamma_{31} = 2\pi\times0.97$ MHz and $\gamma_{21} = 2\pi\times5.9$ MHz, respectively. We assume that the refractive index $n_1 = 1.5$, and the detuning of the coupling field $\Delta_{\mathrm{c}} = 0$. For a cold atomic sample, we assume that the thickness of the sample is half incident probe wavelength, i.e., $L = 490$ nm, the atomic density $N = 6\times10^{15}$ cm^{-3}. For s-polarized incident probe beam, we take that $x_0 = 20$ μm, $a = 0.1$, and lobes develop toward negative x, i.e., $F_0(k') = x_0\exp[\mathrm{i}(k'x_0 + \mathrm{i}a)^3/3]$, the diffraction in medium 1 is $L_{\mathrm{dl}} = k_1x_0^2 \approx 4.8$ mm, and $h = L_{\mathrm{dl}}\cos\theta_1 = 4.8$ mm, 4.73 mm and 4.16 mm are chosen for the probe incidence at $\theta_1 = 0°$, 10° and 30°, respectively.

The propagation of the SR beam for the probe incidence at $\theta_1 = °0$, 10° and 30° are shown on the left panels in Figs. 2(a)~(c), respectively, while the beam amplitudes versus the position χ_{r} from the Snell's reflection axis are shown on the right panels corresponding to each left panel. The maximum value of the first lobe at $z_{\mathrm{r}} = 3$ cm in the right panel in Fig. 2(a) is normalized to 1, and those at $z_{\mathrm{r}} = 0$ in Figs. 2(b) and

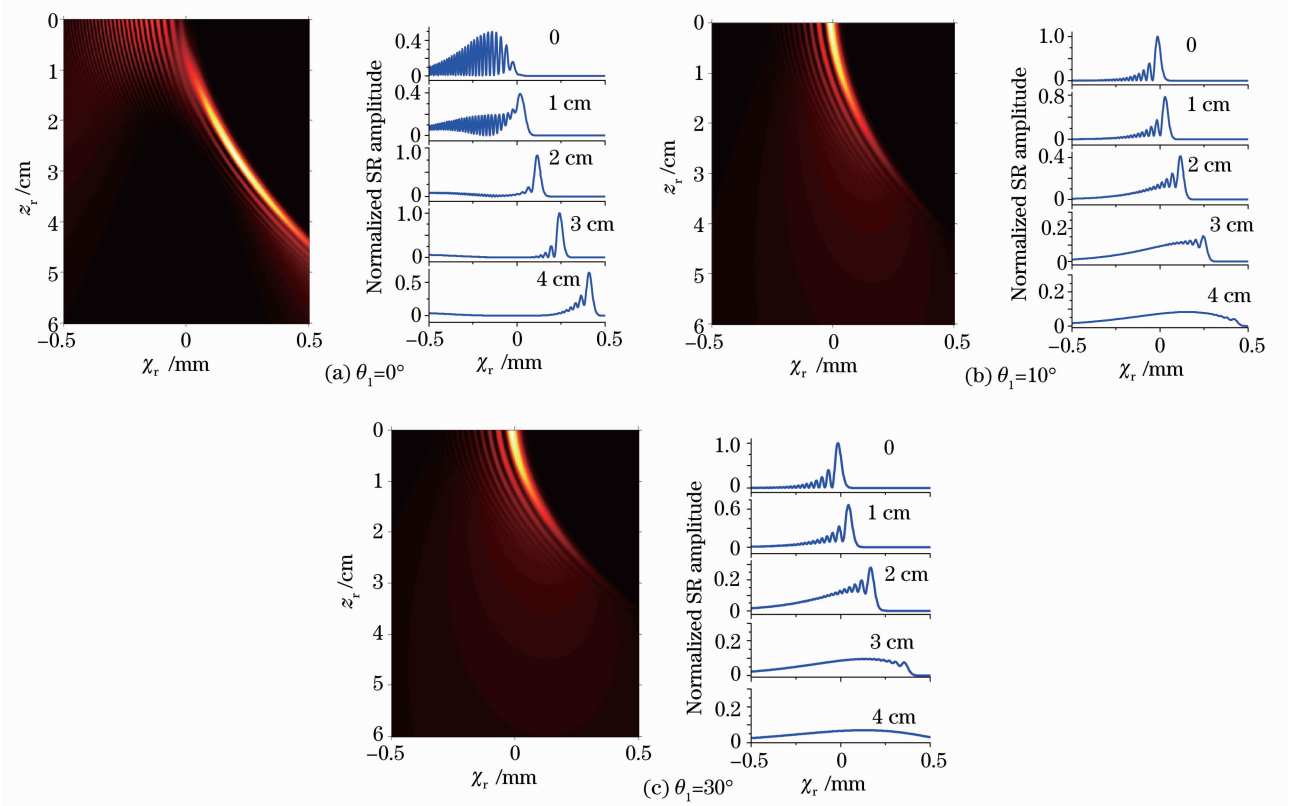

Fig. 2 Left: SR amplitudes of the Airy beams; right: beam amplitudes versus χ_r

(c) are normalized to 1. Other parameters are $G_c = \gamma_{21}$, $\Delta_p = \gamma_{21}$. We find that the SR Airy beams can maintain their properties of resistance to diffraction and self-healing when perturbations from the resonant atoms are imposed on them. It is also shown that the SR beams are quasi-diffraction-free Airy-like beams, which exhibit accelerating dynamics toward the same direction with the incident beam along the Snell's reflection axis, and the larger the incident angle of the probe beam, the greater the accelerating rate of the SR. Self-healing property can be found at both normal and oblique probe incidence, although there is a severe breakdown of that in the former case. These modified SR beams exhibiting various behaviors are due to anisotropic radiation properties along different reflected directions from the resonant atoms.

When the probe incidence is $\theta_1 = 30°$, the amplitudes of the SR beams are plotted for different probe detuning and coupling strengths in Figs. 3(a) and (b), respectively. Thick and thin lines on the left panel for $G_c = \gamma_{21}$ correspond to the probe detuning of $\Delta_p = 0$ (4 times enlarged) and γ_{21}, respectively; the signals are normalized by the maximum value of the first lobe at $z_r = 0$ for $\Delta_p = \gamma_{21}$. While on the right panel, thin and thick lines correspond to $G_c = \gamma_{21}$ and $5\gamma_{21}$ (100 times enlarged), respectively, for a fixed probe detuning $\Delta_p = \gamma_{21}$; the signals are normalized by the maximum value of the first lobe at $z_r = 0$ for $G_c = \gamma_{21}$.

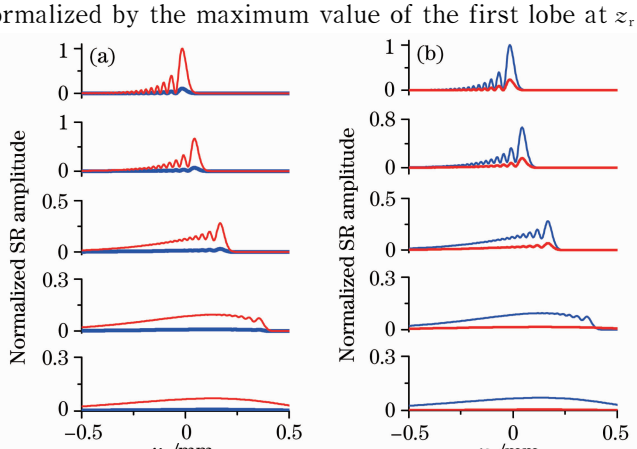

Fig. 3 SR amplitudes for the Airy beam at $\theta_1 = 30°$

It is found that the amplitudes of the SR beams can be dramatically modified by the detuning of the probe field and the strength of the coupling field. This modification can be interpreted by the SR lines plotted in Fig. 4, where solid , dashed , dotted and short-dashed lines correspond to $G_c = 0$, $0.3\gamma_{21}$, γ_{21} and $5\gamma_{21}$, respectively. Each line for $G_c = 0.3\gamma_{21}$, γ_{21} and $5\gamma_{21}$ has a sharp variation of dispersion in the interval $[-G_c, G_c]$, respectively. In these cases, the transmissions are largely enhanced due to EIT effects, leading to a weakened SR. Due to EIT effects induced by the alternating current (AC)-Stark splitting and the interference between dressed states created by a strong coupling field[20-25], the absorption of the probe field is largely suppressed, and the SR from the resonant atoms is very weak for $\Delta_p = 0$ and $G_c = 5\gamma_{21}$ on the left and the right panels, respectively. When the probe detuning $\Delta_p = \gamma_{21}$, or the coupling strength $G_c = \gamma_{21}$, the SR approaches a relatively greater value, since the increased absorption produces a strong reflected radiation. This type of spectrum can probably be used in the detection of resonant properties of particles, as well as the manipulation of the resonant particles near a surface, sensitively.

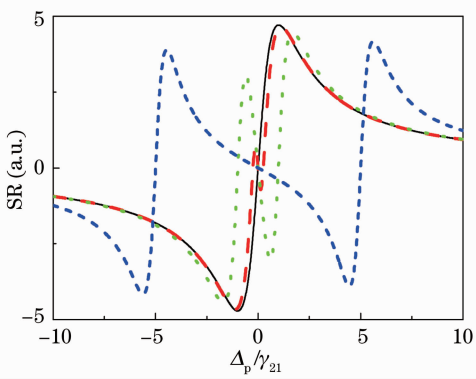

Fig. 4 Real part contribution of SR versus the probe detuning

4 Conclusion

The SR Airy beam from cascade three-level atoms sandwiched between two dielectric walls has been investigated. We show that the SR Airy beams exhibit accelerating dynamics with a parabolic trajectory, and the larger the incident angle of the probe field, the greater the accelerating of the SR beam. Self-healing properties of the SR beams can be found at both normal and oblique probe incidence, although there is a severe breakdown of that in the former case. These various behaviors of the SR beams are due to the contribution of anisotropic radiation along different reflected direction from the resonant atoms.

We also show that the probe detuning and the coupling strength can dramatically modify the amplitudes of the SR beams. Sharp variation of dispersion in the interval $[-G_c, G_c]$ in SR lines indicate greater transmissions of the probe field, and the SR signals are weakened. Due to EIT effects induced by the AC-Stark splitting and the interference between dressed states created by the coupling field, the atomic radiation induced by the probe field is very weak, and the SR from the resonant atoms is largely suppressed for $\Delta_p = 0$ and $G_c = 5\gamma_{21}$ in our discussion. When the probe detuning $\Delta_p = \gamma_{21}$, or the coupling strength $G_c = \gamma_{21}$, the increasing absorption produces a strong reflected radiation, as well as the SR amplitude. This type of Airy beam can probably be used in the detection and the manipulation of resonant particles, as well as the optical storage and communication of information[26,27].

References

1 Siviloglou G, Christodoulides D. Accelerating finite energy Airy beams[J]. Opt Lett, 2007, 32(8): 979-981.

2 Siviloglou G, Broky J, Dogariu A, *et al*.. Observation of accelerating Airy beams[J]. Phys Rev Lett, 2007, 99(21): 213901.

3 Broky J, Siviloglou G, Dogariu A, *et al*.. Self-healing properties of optical Airy beams[J]. Opt Express, 2008, 16(17): 12880-12891.

4 Chu X. Evolution of an Airy beam in turbulence[J]. Opt Lett, 2011, 36(14): 2701-2703.

5 Ren Zhijun, Fan Changjiang, Zhou Weidong. Spatially induced group velocity dispersion of ultrashort pulsed Airy beams[J]. Chinese J Lasers, 2011, 38(12): 1202005.
任志君, 范长江, 周卫东. 超短脉冲艾里光束的空间诱导群速度色散效应研究[J]. 中国激光, 2011, 38(12): 1202005.

6 Zhuang F, Shen J, Du X, *et al*.. Propagation and modulation of Airy beams through a four-level electromagnetic induced transparency atomic vapor[J]. Opt Lett, 2012, 37(15): 3054-3056.

7 Hu Y, Huang S, Zhang P, *et al*.. Persistence and breakdown of Airy beams driven by an initial nonlinearity[J]. Opt Lett,

2010, 35(23): 3952 - 3954.
8 Lin Huichuan, Pu Jixiong. Propagation of Airy beams from right-handed material to left-handed material[J]. Chin Phys B, 2012, 21(5): 054201.
9 Chremmos I, Efremidis N. Reflection and refraction of an Airy beam at a dielectric interface[J]. J Opt Soc Am A, 2012, 29(6): 861 - 868.
10 Yan S, Yao B, Lei M, *et al*.. Virtual source for an Airy beam[J]. Opt Lett, 2012, 37(12): 4774 - 4776.
11 Hu Y, Zhang P, Lou C, *et al*.. Optimal control of the ballistic motion of Airy beams[J]. Opt Lett, 2010, 35(13): 2260 - 2262.
12 Zhang P, Prakash J, Zhang Z, *et al*.. Trapping and guiding microparticles with morphing autofocusing Airy beams[J]. Opt Lett, 2011, 36(15): 2883 - 2885.
13 Polynkin P, Kolesik M, Moloney J, *et al*.. Curved plasma channel generation using ultraintense Airy beams[J]. Science, 2009, 324(5924): 229 - 232.
14 Failache H, Saltiel S, Fichet M, *et al*.. Resonant coupling in the van der Waals interaction between an excited alkali atom and a dielectric surface: an experimental study via stepwise selective reflection spectroscopy[J]. Eur Phys J D, 2003, 23(2): 237 - 255.
15 Chaves de Souza Segundo P, Hamdi I, Fichet M, *et al*.. Selective reflection spectroscopy on the UV third-resonance line of Cs: simultaneous probing of a van der Waals atom-surface interaction sensitive to far IR couplings and interatomic collisions [J]. Laser Phys, 2007, 17(7): 983～992.
16 Laliotis A, Maurin I, Fichet M, *et al*.. Selective reflection spectroscopy at the interface between a calcium fluoride window and Cs vapor[J]. Appl Phys B, 2008, 90(3-4): 415 - 420.
17 Li Yuanyuan, Zhou Yu, Zhang Guizhong. Selective reflection combined with Fabry-Perot effects from two-level atoms confined between two dielectric walls[J]. Chin Phys, 2006, 15(5): 985 - 991.
18 Li Yuanyuan, Hou Xun, Bai Jintao, *et al*.. Two-photon Dicke-narrowing selective reflection spectroscopy in thin atomic vapor[J]. Acta Optica Sinica, 2008, 28(8): 1623 - 1627.
李院院, 侯 洵, 白晋涛, 等. 薄原子蒸气的双光子 Dicke 窄化选择反射光谱到[J]. 光学学报, 2008, 28(8): 1623 - 1627.
19 Li Y, Li L, Lu Y, *et al*.. Selective reflection of Airy beam at an interface between dielectric and homogeneous atomic medium [J]. Opt Express, 2013, 21(7): 8311 - 8318.
20 Scully M, Zubairy M. Quantum Optics[M]. Cambridge: Cambridge University Press, 1997.
21 Harris S. Electromagnetically induced transparency[J]. Phys Today, 1997, 50(7): 36 - 42.
22 Xiao M, Li Y, Jin S, *et al*.. Measurement of dispersive properties of electromagnetically induced transparency in rubidium atoms[J]. Phys Rev Lett, 1995, 74(5): 666 - 669.
23 Fleischhauer M, Imamoglu A, Marangos J. Electromagnetically induced transparency: optics in coherent media[J]. Rev Mod Phys, 2005, 77(2): 633 - 673.
24 Li Xiaoli, Liu Hongna, Yang Yue, *et al*.. Influence of off-resonant coupling field on electromagnetically induced transparency and electromagnetically induced absorption in a closed Λ-shaped four-level system[J]. Acta Optica Sinica, 2011, 31(1): 0102001.
李晓莉, 刘红娜, 杨 悦, 等. 耦合场失谐对闭合 Λ 型四能级系统中电磁诱导透明和电磁诱导吸收的影响[J]. 光学学报, 2011, 31(1): 0102001.
25 Miao Yizhu, Cheng Xuemei, Ren Zhaoyu, *et al*.. Exploration of temperature, power and polarization dependence of four-wave mixing in EIT window[J]. Acta Optica Sinica, 2011, 31(3): 0319001.
苗一珠, 程雪梅, 任兆玉, 等. 电磁诱导透明窗口中温度、功率及偏振特性对四波混频信号的影响[J]. 光学学报, 2011, 31(3): 0319001.
26 Wu Wuming, Ni Yu, Ren Yajie, *et al*.. Research progress of scintillations for laser array beams in atmospheric turbulence [J]. Laser & Optoelectronics Progress, 2012, 49(7): 070008.
吴武明, 宁 禹, 任亚杰, 等. 阵列光束在湍流大气中传输的光强闪烁研究进展[J]. 激光与光电子学进展, 2012, 49(7): 070008.
27 Gan Fuxi, Wang Yang. Breaking through the optical diffraction limits, developing the nano-optics and photonics [J]. Acta Optica Sinica, 2011, 31(9): 0900104.
干福熹, 王 阳. 突破光学衍射极限, 发展纳米光学和光子学[J]. 光学学报, 2011, 31(9): 0900104.